Osteoarthritis and Cartilage 20 (2012) 1258–1267

Osteoarthritis and Cartilage

The extent of degeneration of cruciate ligament is associated with chondrogenic differentiation in patients with osteoarthritis of the knee

K. Kumagai †‡§, K. Sakai †, Y. Kusayama ‡§, Y. Akamatsu ‡§, K. Sakamaki ‖, S. Morita ‖, T. Sasaki ¶, T. Saito ‡§, T. Sakai †#††*

† Department of Biomedical Engineering, Lerner Research Institute, Cleveland Clinic, Cleveland, OH 44195, USA
‡ Department of Orthopaedic Surgery, School of Medicine, Yokohama City University, Yokohama 236-0004, Japan
§ Muscloskeletal Science, Graduate School of Medicine, Yokohama City University, Yokohama 236-0004, Japan
‖ Department of Biostatistics and Epidemiology, Graduate School of Medicine, Yokohama City University, Yokohama 232-0024, Japan
¶ Department of Experimental Medicine I, Nikolaus-Fiebiger Center for Molecular Medicine, University of Erlangen-Nuernberg, Erlangen 91054, Germany
# Orthopaedic and Rheumatologic Research Center, Cleveland Clinic, Cleveland, OH 44195, USA
†† Department of Anatomic Pathology, Pathology and Laboratory Medicine, Cleveland Clinic, Cleveland, OH 44195, USA

ARTICLE INFO

Article history:
Received 20 February 2012
Accepted 18 July 2012

Keywords:
Cruciate ligament
Degeneration
Chondrogenic differentiation
Scleraxis
SOX9
Osteoarthritis

SUMMARY

Objective: Degeneration in cruciate ligaments results from abnormal biomechanical stress and the aging process. Such degeneration is a common outcome in patients with osteoarthritis (OA) of the knee and contributes to the progression of OA. However, to date, there are no specific markers that can predict the extent of ligament degeneration. We hypothesized that the extent of degeneration has correlations to increased chondrogenic potential.

Methods: Twenty anterior cruciate ligaments (ACLs) and 30 posterior cruciate ligaments (PCLs) from 30 knees of 28 adult patients with OA at the time of total knee arthroplasty were used for the study. Degeneration was histologically assessed using a grading system. Expressions of Scleraxis (as a ligament cell marker) and Sry-type HMG box 9 (SOX9) (as a chondrogenic marker) were immunohistochemically assessed in each grade.

Results: We found the opposite expression pattern between Scleraxis and SOX9 according to the grade. The percentage of Scleraxis-positive cells decreased significantly by grade (60.9 ± 23.7 in grade 1, 39.7 ± 30.5 in grade 2, and 13.9 ± 27.1 in grade 3, $P < 0.0001$). In contrast, the percentage of SOX9-positive cells increased significantly by grade (2.5 ± 4.9 in grade 1, 17.5 ± 13.4 in grade 2, and 50.9 ± 27.1 in grade 3, $P < 0.0001$). Furthermore, co-localized expression of both Scleraxis and SOX9 was demonstrated in chondrocyte-like cells.

Conclusions: This study indicates that chondrogenic differentiation is associated with the progression of degeneration in human ligaments. Our results suggest that the expression of SOX9 as a chondrogenic marker could be an indicator for the extent of degeneration in human ligaments. It remains to be elucidated whether suppression of chondrogenic differentiation can prevent progression of the degenerative process of cruciate ligaments in patients with OA.

Introduction

Gradual deterioration of the tissue with corresponding impairment or loss of function is commonly observed in anterior and posterior cruciate ligaments (ACL and PCL, respectively) with osteoarthritis (OA) of the knee[1–4]. Most tendinopathy is associated with degeneration, which is thought to be an active, cell-mediated process involving increased turnover and remodeling of extracellular matrix (ECM)[5]. Such degeneration is thought to contribute to the development of OA[6,7]: for example, aging-related factors contribute to the increased extent of collagen concentration and

Abbreviations: ACL, anterior cruciate ligament; PCL, posterior cruciate ligament; OA, osteoarthritis; ECM, extracellular matrix; SOX9, Sry-type HMG box 9; TKA, total knee arthroplasty; mAb, monoclonal antibody; pAb, polyclonal antibody; DAPI′6-diaminido-2-phenylindole, 4; DAB′3-diaminobenzidine tetrahydrochloride, 3; BSA, bovine serum albumin; PBS, phosphate-buffered saline.

* Address correspondence and reprint requests to: T. Sakai, Department of Biomedical Engineering/ND20, Lerner Research Institute, Cleveland Clinic, 9500 Euclid Avenue, Cleveland, OH 44195, USA. Tel: 1-216-445-3223; Fax: 1-216-444-9198.
E-mail address: sakait@ccf.org (T. Sakai).

1063-4584/$ – see front matter © 2012 Osteoarthritis Research Society International. Published by Elsevier Ltd. All rights reserved.
http://dx.doi.org/10.1016/j.joca.2012.07.013

decreased collagen fibril diameters in cruciate ligaments[8]. Although loss of joint stability in cruciate ligaments is a risk factor for OA[9,10] and severe degeneration of the ACL is more common in high-grade than low-grade OA[11], the biological mechanisms underlying ligament degeneration have not been well characterized.

Histologically, degeneration of ligaments is in general characterized by disorganization of collagen fiber arrangement, mucoid changes, chondroid metaplasia, and cystic changes[7,11,12]. Morphologically, degenerating ligament cells undergo chondrocyte-patterns such as large round nuclei and/or cells with lacunae. Alterations in collagen composition, including accumulation of collagen type III and induction of collagen type II in the fibrocartilaginous regions, are also observed in ruptured or degenerating ligaments[13,14].

Scleraxis, a basic helix-loop-helix transcription factor, has been identified as a specific marker of tenogenic cells and mature differentiated tenocytes[15–17]. We have shown that mechanical forces at physiological levels play a critical role in maintaining the expression of Scleraxis in adult tendon cells through TGF-β/Smad2/3-mediated signaling[18]. However, it remains unknown whether the expression of Scleraxis in ligaments is altered according to the extent of degeneration. Furthermore, no studies have addressed whether cells displaying chondrogenic patterns in degenerating ligaments induce Sry-type HMG box 9 (SOX9), which is specifically expressed in chondrocytes[19]. We hypothesized that cells in degenerating ligaments acquire a chrondrogenic potential, thereby resulting in the downregulation of Scleraxis and upregulation of SOX9 expression. Here we show persuasive evidence of chondrogenic differentiation with the degenerative process in cruciate ligaments.

Materials and methods

Subjects

Twenty ACLs and 30 PCLs were harvested from 30 knees of 28 patients with OA who underwent posterior stabilized total knee arthroplasty (TKA). The patients comprised 23 female and five male patients (mean age, 77 years; range, 67–84 years). According to the radiographic grading for osteoarthritic knees[20], 10 knees were grade 3, 14 knees were grade 4, and six knees were grade 5. Twenty-six knees had varus deformity (femorotibial angle $= 186.3 \pm 4.9^{\circ}$), and four knees had valgus deformity (femorotibial angle $= 169.3 \pm 7.8^{\circ}$). Patients who had a history of knee injury, previous knee surgery, inflammatory arthritis, joint infection, or immunosuppression therapy were excluded from the study. The present study was approved by the Institutional Review Board at the hospital where the TKAs were performed, and informed consent was obtained from all patients.

Generation of antibody against Scleraxis

DNA coding mouse *scleraxis* residues (the N-terminal region before the basic DNA-binding domain) were obtained by PCR using from whole *scleraxis* cDNA (pcDNA-SCX, kindly provided by Dr. Véronique Léjard). We used the N-terminal region before the basic DNA-binding domain to generate antibody to prevent potential cross-reactions of antibody with other basic helix-loop-helix transcription factors. The oligonucleotide primers introduced an *Nde*I site at the 5′-end and a *Bam*HI site at the 3′-end to allow insertion into the pET15b vector (Novagen). The correct sequence was confirmed by DNA sequencing. An expression vector was used for the transformation of *E. coli* BL21 (DE3: Novagen). A bacterial pellet was suspended in 8 M urea/10 mM Tris/100 mM sodium phosphate, pH 8.0, and the recombinant protein was purified using Ni-NTA agarose according to the manufacturer's instructions (QIAGEN). Immunization of rabbits and affinity-purification of antibodies followed standard protocols[21].

Isolation of primary tenocytes from adult mouse tendons and generation of Scleraxis-null and Scleraxis-expressing tenocyte lines

Although Achilles tendon is the most commonly used tendon tissue for research in the adult mouse and has the largest fibrous tissue structure available for analysis, a typical yield of approximately 1.5×10^4 cells per sample made it impractical to carry out biochemical observations such as Western analysis[18]. Therefore, we generated Scleraxis-null and Scleraxis-overexpressing tendon lines. Isolation of tenocytes and establishment of tenocyte cell lines were described previously[18]. Briefly, Scleraxis-null tendon cell lines were generated from Achilles tendon of adult mice on *Scleraxis(fl/fl)/p53*- and *Scleraxis(fl/fl)p21*-null genetic background. Those cells were isolated and cloned, and several immortalized clones were generated. Subsequently, several clones were treated with a *Cre*-transducing adenovirus to delete the *Scleraxis-floxed* genes as described[22]. The deletion of *Scleraxis* alleles was confirmed by PCR (*Scleraxis(fl/fl)* mice were kindly provided by Dr. Ronen Schweitzer[23]). For inactivation Scleraxis gene in adult mice, we performed a single injection of adenovirus encoding *Cre* recombinase into the Achilles tendon of adult *Scleraxis(fl/fl)* mice and wild-type mice[24,25]. One week later, the expression of Scleraxis protein in tenocytes was evaluated by immunohistochemistry.

To generate Scleraxis-expressing tenocyte lines, we generated a Scleraxis and Flag-tag fusion protein expression construct. Flag-tag was inserted at the N-terminal site (upstream of the start codon) or C-terminal site (upstream of the stop codon) of cDNA encoding Scleraxis and cloned in lentiviral pCDH-CMV-MCS1-Puro expression vector (pCDH-CMV-MCS-Puro_ScleraxisFlag, System Biosciences). We used murine cDNA to characterize the specificity of the antibody using mouse Scleraxis protein. The sequence homology between mouse and human Scleraxis cDNA used for antibody preparation is almost identical (>94% homology): there is only one amino acid-difference and murine cDNA has three additional amino acids. For lentivirus production, HEK293T cells were transfected with pCMV-VSV-G (Addgene plasmid 8454), pCMV-dR8.2 dvpr (Addgene plasmid 8455), and pCDH-CMV-MCS-Puro_ScleraxisFlag or pCDH-CMV-MCS-Puro (mock) using lipofectamine (Invitrogen)[26]. Then lentiviral infection was performed in Scleraxis-null tendon cells. To generate stable clones, selection with 10 μ/ml puromycin was started at 72 h after transfection, and the surviving clones were isolated and expanded.

Antibodies and reagents

The following antibodies were used for the analyses: mouse monoclonal antibody (mAb) against Flag M2 (Sigma, St. Louis, MO, USA); rabbit polyclonal antibody (pAb) against Scleraxis (described above); rabbit pAb against SOX9 (Millipore, Temecula, CA, USA); rabbit pAb against type I collagen (Calbiochem, San Diego, CA, USA), rabbit pAbs against type II and type III collagen were generated according to the standard protocols[22]; rabbit pAb against aggrecan (Chemicon, Temecula, CA, USA); normal rabbit IgG (Santa Cruz Biotechnology, Santa Cruz, CA, USA); biotinylated donkey anti-rabbit IgG and Cy3-conjugated donkey anti-rabbit IgG (Jackson ImmunoResearch Laboratories, West Grove, PA, USA). The following reagents were used for the analyses: Vectastain ABC Kit, Vector ImmPACT VIP substrate kit, and mounting medium containing 4′6-diaminido-2-phenylindole (DAPI) (Vector Laboratories, Burlingame, California, USA); 3′3-diaminobenzidine tetrahydrochloride

(DAB) (Dojindo, Kumamoto, Japan); pepsin (P-7000) and hyaluronidase (Sigma); chondroitinase ABC (Seikagaku Co., Tokyo, Japan).

Western blot analysis

For immunoblotting analyses, samples were transferred onto Immobilon-FL PDVF membrane (Millipore Corp.) and probed with primary and IRDye 800CW- or IRDye 680-conjugated secondary antibodies (LI-COR Biosciences, Lincoln, NE, USA). Immunoreactive bands were detected using the Odyssey Infrared Imaging System (LI-COR) as described previously[22].

Sample preparation and histological analysis

The midvastus muscle-splitting approach was performed through a standard anterior midline skin incision for the TKA. Before resection of the cruciate ligaments, intra-operative macroscopic assessment of the ACL and the PCL was performed by the surgeon. Three grades of macroscopic appearance were identified as previously described[2]: grade 0, normal; grade 1, abnormal (thinner than normal and sclerotic); or grade 2, ruptured (complete disappearance of the ligament, which is destroyed, or persistence of only a few fibers). Cruciate ligaments were excised from the tibial and femoral attachments. Although there are differences in the length, thickness, and geometry between ACL and PCL[27], their histological structure (including collagen fibril diameter)[28,29] and cellular phenotypes[30] are quite similar. Therefore, both ACL and PCL were used for the microscopic analysis. Each insertion site was removed and we got the mid portion of ligaments, and preserved immediately in 10% neutral buffered formalin. Half of each ligament sample was then dehydrated in ascending series of ethanol and embedded in paraffin. The other half was frozen in an optimum cutting temperature (OCT) compound and stored at −80°C. Paraffin-embedded samples were sectioned longitudinally (5 μm thick). The sections were stained with hematoxylin/eosin or Alcian blue according to the standard protocols. The process of sample preparation is summarized in Fig. 1.

Immunohistochemical analysis

For immunohistochemistry, paraffin sections were permeabilized with 0.2% Triton X-100 for 5 min after the deparaffinization step. Endogenous peroxidase was quenched for 10 min with 3% H_2O_2 in water. Nonspecific binding was blocked with 3% bovine serum albumin (BSA) in phosphate-buffered saline (PBS). Anti-Scleraxis or anti-SOX9 antibody was incubated overnight at 4°C. The next day, slides were washed in PBS and incubated with biotinylated anti-rabbit IgG antibody for 45 min at room temperature. Reaction was visualized by incubation with the avidin–biotin–peroxidase reagent included in the Vectastain ABC Kit followed by color development with DAB. Finally, the sections were counterstained with hematoxylin and mounted with coverslips. Normal rabbit IgG was used for negative control [Fig. 2(C)].

Double-immunohistochemical analysis was performed as described[22]. Briefly, the first antigen-antibody reaction using anti-Scleraxis antibody was carried out, and color development was performed with DAB. The slides were incubated with dissociation buffer containing 0.1 M glycine–HCl (pH 2.2) to dissociate immunoglobulins from antigenic sites. Then the second antigen-antibody reaction using anti-SOX9 antibody was carried out, and color development was performed with Vector ImmPACT VIP. We performed the same staining in reverse order, first SOX9, then Scleraxis, and confirmed the same double-positive findings. We carried out the second antigen-antibody reaction without antibodies and confirmed the complete dissociation of the first immunoglobulins.

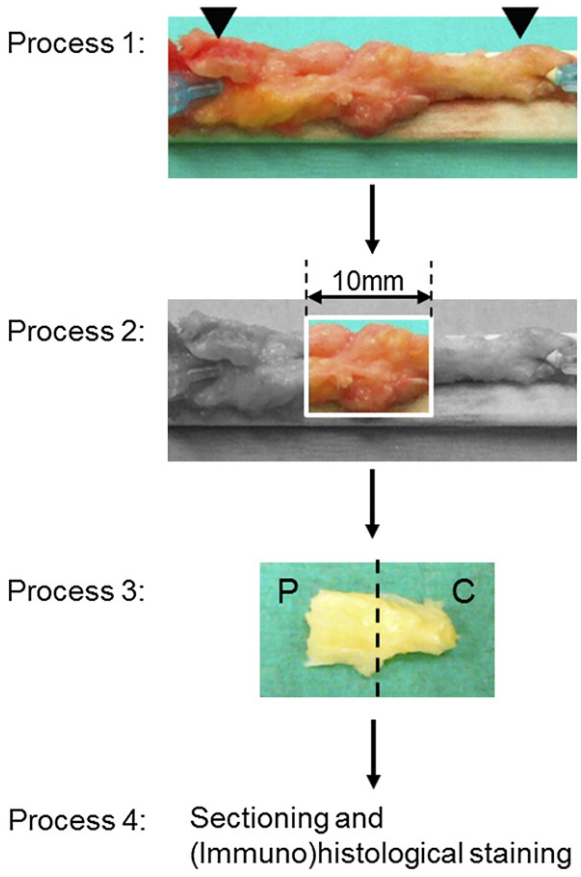

Fig. 1. The process of sample preparation. Process 1: Cruciate ligaments were excised from the tibial and femoral attachments (arrowheads). Process 2: Each insertion site was removed and the mid portion of the ligament (highlighted box) was obtained. Process 3: The mid portion of the ligament was divided into two tissue fragments: one was for the preparation of paraffin sections (P), the other was for cryosections (C). Process 4: Longitudinal sections obtained from paraffin- and OCT-embedded samples were used for (immuno)histological stainings: Hematoxylin/eosin, Alcian blue, Scleraxis, SOX9, and Scleraxis–SOX9 double stainings were performed using paraffin-embedded tissue sections, and type I, type II, and type III collagen, and aggrecan stainings were performed using OCT-embedded frozen tissue sections. Each staining was performed using at least five sections in each sample.

For immunofluorescence, longitudinal cryosections (5 μm of thick) were prepared and washed with PBS. Antigen retrieval was performed by incubation with 0.2% pepsin in 0.01 N HCl for 30 min at 37°C prior to applying type I collagen antibody, 1 mg/ml hyaluronidase in PBS (pH 5.0) for 30 min at room temperature prior to applying type II collagen antibody, or 1 U/ml chondroitinase ABC in 20 mM Tris–HCl buffer solution (pH 8.0) for 2 h at 37°C prior to applying aggrecan antibody. After blocking of nonspecific binding with 3% BSA in PBS, primary antibody was incubated for 1 h at room temperature. Then slides were washed in PBS and incubated with Cy3-conjugated donkey anti-rabbit IgG. The slides were mounted with DAPI to stain the nucleus.

Evaluation of degeneration in cruciate ligaments

Five high-power fields per each section were randomly captured using a Leica DMR microscope, with a Qimaging Retiga EXi cooled CCD camera (Q-Imaging Inc., Burnaby, BC, Canada). Each field was assessed by cellular arrangement and morphological change of cell nuclei. Following three-point scoring system was used in two variables with a modification of previously described methods[11,12,31,32]:

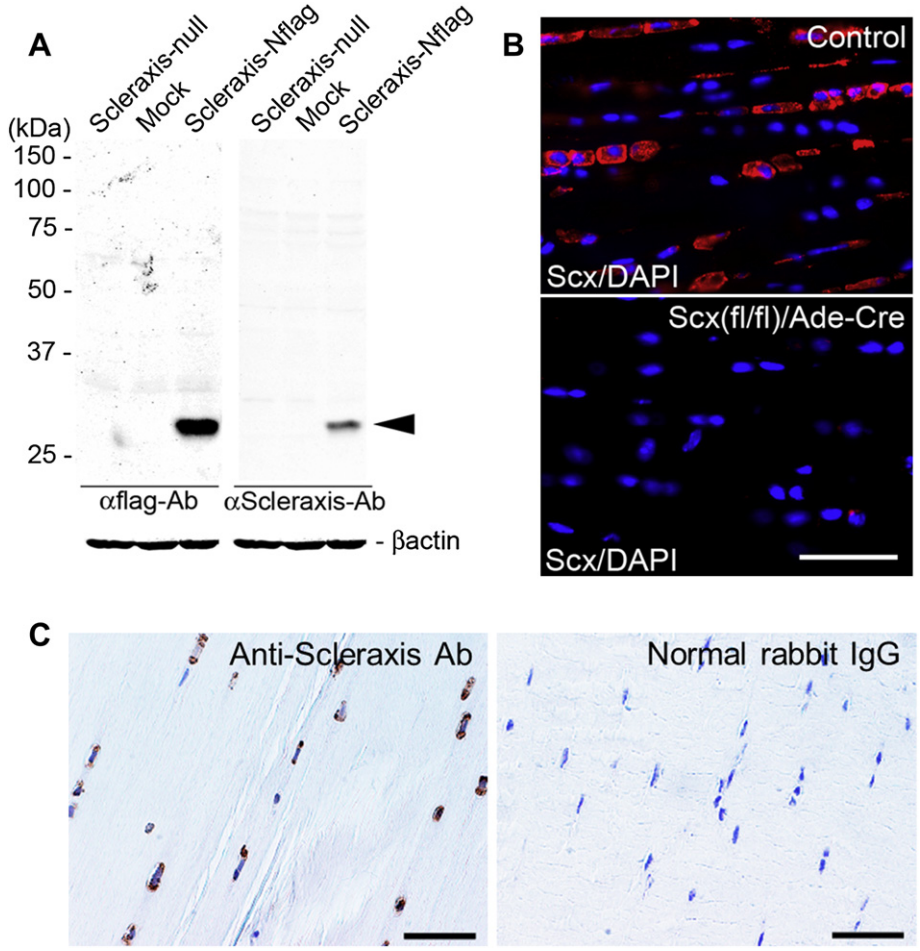

Fig. 2. Specificity of Scleraxis antibody. (A) Western blot analysis of lysates from Scleraxis-null, mock-transfected, and Scleraxis/N-terminal flag fusion protein transfected cells. The position of a molecular mass marker (kDa) is indicated. β-actin served as a loading control. (B) Immunofluorescence staining for Scleraxis of the Achilles tendon in wild-type (upper panel) and *Scleraxis(fl/fl)* (lower panel) mice at 7 days after local injection of adenovirus-Cre (red, Scleraxis; blue, DAPI). Scale bar = 50 μm. (C) Immuohistochemical stainings in human cruciate ligament using anti-Scleraxis antibody (left panel) and normal rabbit IgG (right panel, as a negative control). Note that no background staining is confirmed in the section using normal rabbit IgG. Scale bar = 25 μm.

For the assessment of cellular arrangement:

The angles between the long axis in each cell and the direction of collagenous fibers were measured. The scoring point in each field was determined as follows:

Point 0: less than 10 degrees of alignment in all cells examined.
1: 11–45 degrees of alignment in less than 50% cells and less than 10 degrees of alignment in the rest.
2: over 10 degrees of alignment in more than 50% cells or existence of cells with over 45 degrees of alignment.

In case of completely round cells, we could not define a cellular axis and scored such cells as point 2. We also scored point 2 when the fiber direction was lost.

For the assessment of morphological changes in the cell nuclei:

Point 0: no appearance of round nuclei.
1: <50% appearance of round nuclei.
2: ≥50% appearance of round nuclei.

When 0 points were scored in both variables or 1 point was scored in either of the variables, the field was defined as grade 1. When abnormal changes (1 or 2 points) were scored in both variables and 2 points were scored in at least 1 variable, the field was defined as grade 3. Consequently, each field was graded by the total score: Total score 0 or 1 = grade 1; Total score 2 = grade 2; Total score 3 or 4 = grade 3. For the assessment of degenerative grade, we examined at least five different high-power fields in each ligament and calculated each parameter: all cells in each field were analyzed for cell density, cellular arrangement, and morphological changes. Two independent observers assessed degenerative grade. The kappa coefficient value in the grading score was 0.79, indicating good agreement for inter-observer reproducibility.

Quantification of labeled cells

The number of total cells and Scleraxis- and SOX9-positive cells were counted, then the positive cell ratio was calculated in each field. The results were compared among the grades of degeneration.

Statistical analysis

The mixed-effects model was used to investigate the relationship of the cell density and the markers with the grade because of the non-independence of the multiple measurements from the same patient. When a significant difference of the cell density among the grades was detected by the mixed-effects model, the

Tukey–Kramer *post hoc* all-pairwise tests of the means were performed. To confirm the linear relationship between the grade and the markers, we tested the slope of the grade as a continuous variable in the mixed-effects model. A chi-square test was performed to analyze the distribution of grades between ACL and PCL. P value < 0.05 was considered statistically significant. All data were expressed as mean ± standard deviation (SD). Analysis was done using SigmaStat 3.5 software (Systat Software Inc., Richmond, CA, USA) and SAS 9.3 (SAS Institute Inc., Cary, NC, USA).

Results

Specificity of Scleraxis antibody

We first characterized our Scleraxis antibody by Western analysis. Scleraxis antibody did react with lysates from cells expressing Scleraxis/N-terminal flag fusion proteins with an apparent molecular mass of ~30 kDa under reducing conditions, but it did not react with lysates from Scleraxis-null or mock-transfected cells [Fig. 2(A)]. Furthermore, the molecular size of the reacted band was completely identical to that detected with anti-flag antibody from cells expressing Scleraxis/N-terminal flag fusion proteins [Fig. 2(A), arrowhead]. Immunofluorescence analysis of adult mouse Achilles tendons further confirmed considerably decreased expression of Scleraxis in *Cre*-treated *Scleraxis(fl/fl)* tendon cells, whereas intense Scleraxis protein expression was evident in wild-type tenocytes [Fig. 2(B)]. These findings indicate that our Scleraxis antibody specifically detects Scleraxis proteins.

Macroscopic appearance of cruciate ligaments in arthritic knees

We obtained 20 ACLs and 30 PCLs. Macroscopic findings are summarized in Table I. They consisted of nine normal, 11 thin and sclerotic, and 10 ruptured samples from ACLs; 22 normal, and eight thin and sclerotic samples from PCLs. There were no macroscopically ruptured PCLs on intra-operative inspection. Ruptured ACLs in 10 knees were excluded from this study due to complete loss of the ligament or persistence of only a few fibers.

Histology of degenerating cruciate ligament

For histological evaluation, each field was graded in terms of cellular alignments, and cellular shapes (i.e., spindle or round) [Fig. 3(A), Table II]. Cruciate ligaments obtained from OA patients revealed a highly variable collagen fiber arrangement and cellular morphology. Thirty-seven of 250 fields (14.8%) were classified as grade 1, characterized with parallel fiber arrangement, including 82% of spindle-shaped cell nuclei. Eighty-seven fields (34.8%) were classified as grade 2 and 126 fields (50.4%) were classified as grade 3. ACL consisted of 12% grade 1, 36% grade 2, and 52% grade 3, and PCL consisted of 17.3% grade 1, 33.3% grade 2, and 49.3% grade 3. There were no significant differences of grade distribution between ACL and PCL ($P = 0.57$, chi-square test). As the grade increased, collagenous fibers lost the orientation of parallel alignment, and nuclei became round, revealing the possible chondrogenic differentiation. Cruciate ligaments in grade 3 almost completely lost parallel fiber arrangement, and round cell shapes with round nuclei resembling those of chondrocytes were often observed.

Table I
Classification of grades according to macroscopic findings of cruciate ligaments in OA knees

Grade	ACL	PCL
0 (Normal)	9 (30)	22 (73.3)
1 (Abnormal)	11 (36.7)	8 (26.7)
2 (Ruptured)	10 (33.3)	0 (0)

Values represent the number of knees and (%).

Next, cell density in each grade was calculated to assess the number of cells (Table II). The mean cell density was 349 ± 179/mm^2 in grade 1 ($n = 37$), 460 ± 328/mm^2 in grade 2 ($n = 87$), and 361 ± 199/mm^2 in grade 3 ($n = 126$). The statistical tests using a mixed-effects model and a *post hoc* all-pairwise multiple comparison showed a significant difference between grades 2 and 3 ($P < 0.05$, Tukey–Kramer test).

Immunofluorescence of collagen type I and III

To assess collagen content in ECM associated with degeneration, we examined localization of collagen type I and III by immunofluorescence findings [Fig. 3(B)]. The collagen type I, a predominant constituent in tendons/ligaments[5], was confirmed in most of the ECM. The prevalence of collagen type I was similar among grades. The deposition of collagen type III was sometimes observed as foci in the ECM surrounding round cells in early stages of degeneration, and this deposition of collagen type III was preserved in advanced stages of degeneration, suggesting active remodeling reactions in these cells during chronic degeneration process[5].

Immunohistochemical analysis of Scleraxis

To identify expression of tendons/ligaments specific marker in degenerating cruciate ligaments, we performed immunostaining for Scleraxis. Each image was graded, and the number of Scleraxis-positive cells was measured [Fig. 4(A)]. The percentage of Scleraxis-positive cells/total cells in each grade was 60.9 ± 23.7% in grade 1 ($n = 47$), 39.7 ± 30.5% in grade 2 ($n = 105$), and 13.9 ± 27.1% in grade 3 ($n = 98$) ($P < 0.0001$ among grades), and decreased according to the grade of degeneration (slope, −17.3; $P < 0.0001$) [Fig. 4(B), left]. Of the Scleraxis-positive cells, 65.2% had spindle-shaped nuclei and 34.8% had round nuclei. Furthermore, the compositions of spindle-shaped vs round nuclei in each grade were 83.5%/16.5% in grade 1 ($n = 46$), 64.9%/35.1% in grade 2 ($n = 77$), and 50.9%/49.1% in grade 3 ($n = 49$) (slope, 16.1; $P < 0.0001$) [Fig. 4(B), right]. These findings revealed that the ratio of round nuclei in Scleraxis-positive cells increased with grade of degeneration, suggesting possible sustained expression in early stages of the chondrogenic differentiation process.

Immunohistochemical analysis of SOX9

To investigate the chondrogenic potential in degenerating cruciate ligaments, we performed immunostaining for SOX9. Each field was graded, and the number of SOX9-positive cells was measured [Fig. 4(C)]. The percentage of SOX9-positive cells/total cells was 2.5 ± 4.9% in grade 1 ($n = 44$), 17.5 ± 13.4% in grade 2 ($n = 79$), and 50.9 ± 27.1% in grade 3 ($n = 127$) ($P < 0.0001$ among grades), and increased according to the grade of degeneration (slope, 22.5; $P < 0.0001$) [Fig. 4(D), left]. Expression of SOX9 was observed in 21.0% of cells with spindle-shaped nuclei and 79.0% of cells with round nuclei. Of the SOX9-positive cells, the compositions of spindle-shaped vs round nuclei in each grade were 62.8%/37.2% in grade 1 ($n = 14$), 31.4%/68.6% in grade 2 ($n = 66$), and 16.1%/83.9% in grade 3 ($n = 121$) (slope, 17.3; $P < 0.0001$) [Fig. 4(D), right].

Co-localized expression of Scleraxis and SOX9

To examine whether ligament cells expressing Scleraxis have chondrogenic potential, we performed double-immunohistochemical staining for Scleraxis and SOX9. Co-localized expression of both

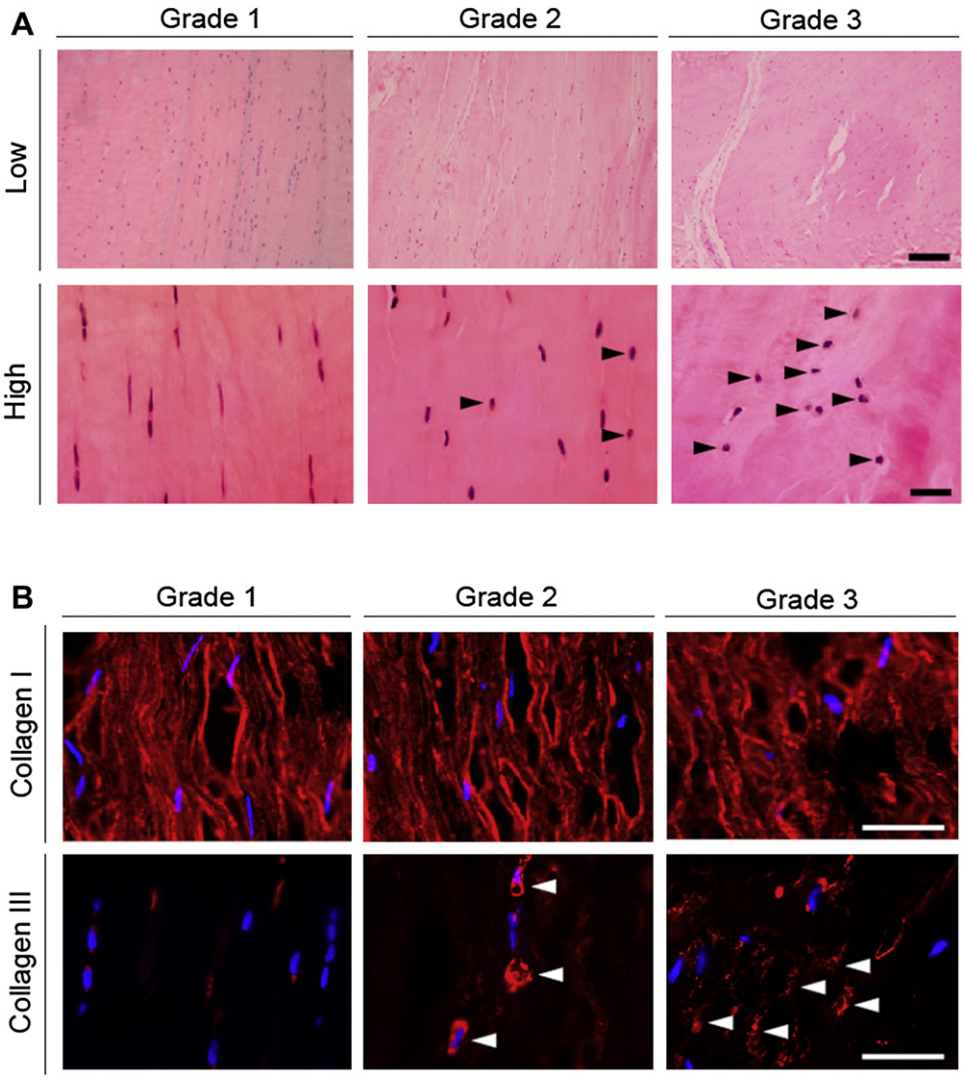

Fig. 3. Representative histopathological findings in degenerating cruciate ligaments. (A) Typical morphological patterns in grade 1–3. Grade 1 represents normal or slight degeneration, and grade 3 represents most advanced degeneration. Parallel cellular arrangement reduces but the number of cells with round nuclei (arrowheads) increases in accordance with the grade of degeneration. Hematoxylin/eosin staining. Upper panels: low magnification. Scale bar = 100 μm. Lower panels: higher magnification. Scale bar = 25 μm. (B) Immunofluorescence staining for collagen type I and III in grades 1–3. Upper panels: collagen type I (red) and nuclear staining with DAPI (blue). The tissue distribution of collagen type I is similar in each grade. Lower panels: collagen type III (red) and DAPI (blue). Foci of collagen type III are shown surrounding round cells in grade 2 (arrowheads), and several deposition foci are preserved in the ECM in grade 3 (arrowheads). Scale bar = 25 μm.

Scleraxis and SOX9 was often demonstrated in chondocyte-like cells (Fig. 5).

Immunofluorescence of collagen type II and aggrecan

To further address the chondrogenic potential in degenerative ligaments, we examined the deposition of collagen type II, a major component of cartilage ECM. Focal and scattered spot-like depositions of collagen type II were found in the ECM surrounding round cells with round nuclei [Fig. 6(A), upper panels]. Weak expression of aggrecan was also observed in the ECM surrounding those round cells [Fig. 6(A), lower panels]. These deposition and localization patterns of collagen type II and aggrecan suggest that a chondrogenic potential was induced in the ECM with increasing degeneration. In addition to identification of collagen type II and aggrecan, Alcian blue-positive areas were found in the ECM surrounding the round cells, confirming the accumulation of glycosaminoglycans [Fig. 6(B)].

Table II
The number of assigned fields and the mean cell density in each histological grade of cruciate ligaments

	Grade 1	Grade 2	Grade 3
Number of fields	37 (14.8%)	87 (34.8%)	126 (50.4%)
Cell density (cells/mm^2)*	349 ± 179	460 ± 328†	361 ± 199†

* Values represent mean ± SD.
† Significant difference between grade 2 and grade 3 ($P < 0.05$).

Discussion

The major advances in the present study are the assessment of a relationship between 1) the histological grade of degeneration and chondrogenic differentiation with the specific marker SOX9, and 2) the histological grade of degeneration and Scleraxis expression levels. We have demonstrated decreased numbers of Scleraxis-positive cells and increased numbers of SOX9-positive cells according to the histological grade of degeneration. We

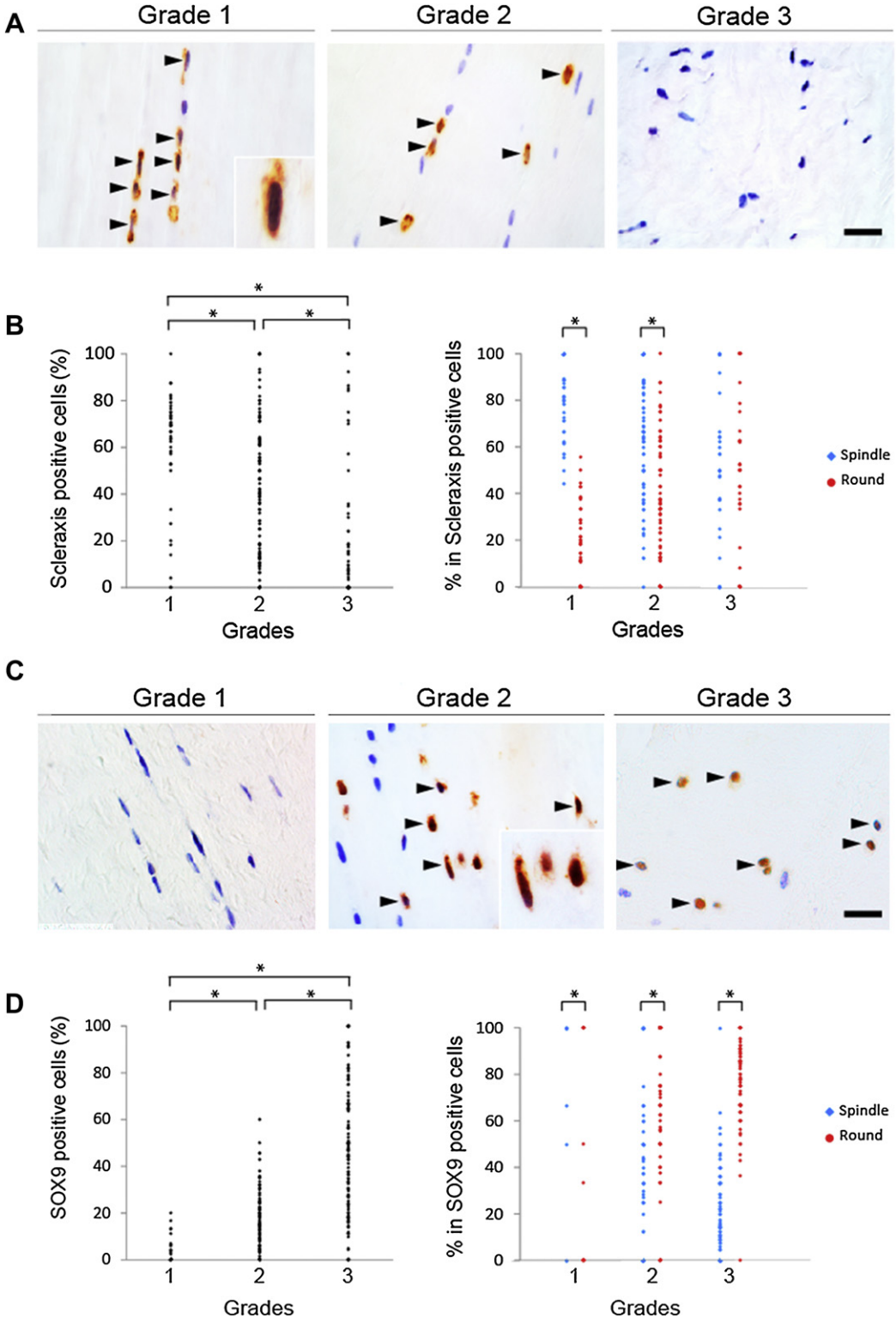

Fig. 4. Expression patterns of Scleraxis and SOX9 in each grade of degeneration. (A, B) Immuohistochemical staining for Scleraxis in grades 1–3. (A) Arrowheads indicate Scleraxis-positive cells (brown). Scale bar = 25 μm. Note that positive staining is shown in both nucleus and cytoplasm (inset). (B) Left panel: percentage of Scleraxis-positive cells. Grade 1; $n = 47$, grade 2; $n = 105$, grade 3; $n = 98$. Values are given as mean ± SD. Right panel: percentage of spindle-shaped/round nuclei in Scleraxis-positive cells. Grade 1; $n = 46$, grade 2; $n = 77$, grade 3; $n = 49$. Values are given as mean ± SD. $^*P < 0.05$. (C, D) Immunohistochemical staining for SOX9 in grades 1–3. (C) Arrowheads indicate SOX9-positive cells (brown). Scale bar = 25 μm. Note that positive staining is shown in both nucleus and cytoplasm (inset). (D) Left panel: percentage of SOX9-positive cells. Grade 1; $n = 44$, grade 2; $n = 79$, grade 3; $n = 127$. Values are given as mean ± SD. Right panel: percentage of spindle-shaped/round nuclei in SOX9-positive cells. Grade 1; $n = 14$, grade 2; $n = 66$, grade 3; $n = 121$. Values are given as mean ± SD. $^*P < 0.05$.

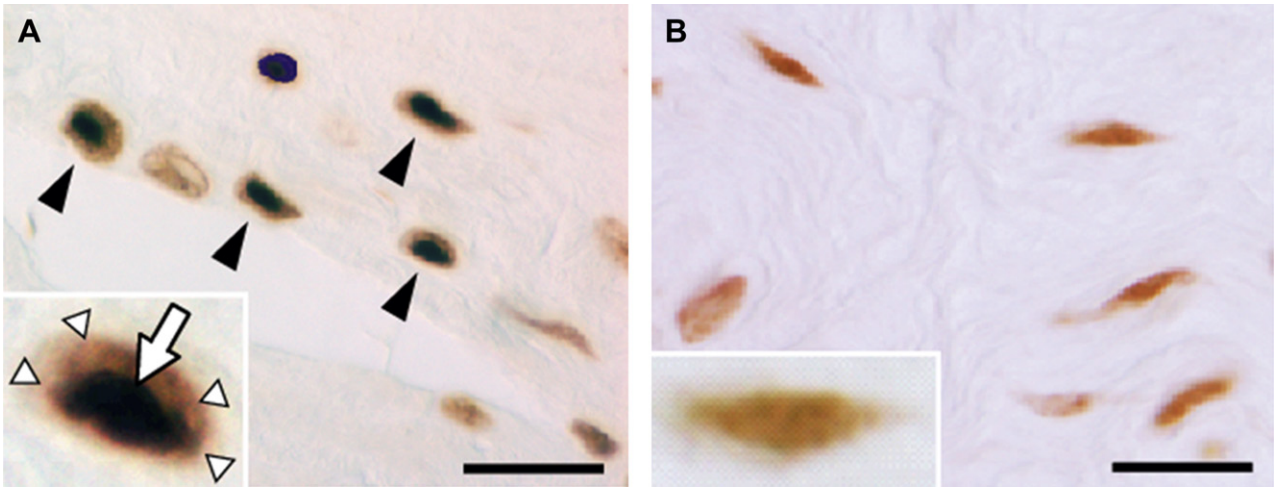

Fig. 5. Co-localized expression of Scleraxis and SOX9. (A) Double-immunohistochemical staining for Scleraxis and SOX9 (from grade 2 sample). Scleraxis (light brown) is co-localized with SOX9 (dark purple) in chondrocyte-like cells (black arrowheads). Scale bar = 25 μm. Inset: cellular co-localization of Scleraxis (white arrowheads) and SOX9 (white arrow). (B) The same staining procedures shown in (A) without second antigen-antibody reaction (from grade 2 sample). Positive cells express only Scleraxis (light brown) as the first antigen-antibody products. Scale bar = 25 μm. Inset: cellular distribution of Scleraxis (both nucleus and cytoplasm).

propose that such alterations account for chondrogenic differentiation of cells in degenerative ligaments.

Several studies indicate structural/morphological changes in degenerative human ligaments: they show the disorganization of fiber arrangements and the presence of chondrocyte-like cells[7,11,12,33]. Indeed, in tendon degeneration models such as the rat collagenase-induced patellar tendon degeneration model, approximately 5% of degenerating areas show calcific foci, in which chondrocyte-like cells expressing collagen type II and SOX9 are observed around those foci[19]. However, to date, no studies have shown alterations in expression profiles of ligament and chondrocyte markers in those cells during the progression of ligament degeneration. Here we have provided evidence that the number of SOX9-positive chondrocyte-like cells actually increase significantly according to human ligament degeneration with cartilage-specific collagen type II and aggrecan depositions. Thus, our findings suggest that chondrogenic differentiation may play a key role in the progression of ligament degeneration and that the number of SOX9-positive cells could be a potential indicator to determine the extent of degeneration in ligaments.

We suggest possible mechanisms for decreased number of Scleraxis-positive cells in degenerative ligaments. First, there is evidence that the expression of Scleraxis depends on the levels of physical forces: the loss of tensile loading from skeletal muscles in the mouse Achilles tendon complete transection model immediately and significantly downregulates Scleraxis expression in tendon cells[18]. Furthermore, several studies using intact human knees (femur-ACL-tibia complex) have shown that the biomechanical properties of the knees such as strength and stiffness, are significantly reduced with increasing age[34,35]. Although no studies have demonstrated direct evidence showing decreased biomechanical properties in degenerative ligaments, these findings suggest that both aging and alterations of physical forces could contribute to the downregulation of Scleraxis expression and the degenerative process in ligaments. Secondly, decreased cellular densities are observed in advanced human rotator cuff degeneration, and apoptosis plays an important role in this degenerative process[31,36]. Therefore, as we previously found in mouse tendon injury models[18], it is likely that the downregulation of Scleraxis expression levels can contribute to a cell-death cascade in degenerative ligaments.

Recent findings from developing embryos illuminate the reciprocal interactions among the forming tendon/ligament, muscle and cartilage tissues[37,38]. Although chondrogenic differentiation is regulated by the interaction between Scleraxis and SOX9[39], several studies show functional correlations between the loss of Scleraxis and the upregulation of SOX9 in the transdifferentiation of ligament/tendon cells to chondrocyte-like cells: cultured ACL-derived cells acquire a chondrogenic property with SOX9 expression under chondrogenesis-induction medium[40]. Moreover, Takimoto *et al.*[41] have demonstrated that overexpression of SOX9 induced the direct conversion of tenocytes into chondrocytes with down-regulation of Scleraxis expression *in vitro*. Thus, the loss of Scleraxis-positive cells in degenerative ligaments may be due to transdifferentiation of tendon cells into chondrocyte-like cells. Importantly, we have demonstrated in the present study the cells expressing both Scleraxis and SOX9 in degenerative human ligaments, which suggests that even mature ligament cells have a chondrogenic potential with the process of degeneration.

One limitation of this study could be the absence of normal samples (no degenerative changes). The mean age of subjects in the present study is relatively old (77 years, range 67–84). Indeed, the extent of degeneration in cruciate ligaments increases with age[7]. Therefore, even if we obtained samples from healthy people of the same age as those in the present study, they could not be used as normal controls. The focus of the current study is to identify the variation of cellular events with degeneration, and the results presented here are sufficient to justify our conclusions.

This study provides insights into the modulation of Scleraxis and SOX9 expression in the process of ligament degeneration. Chondrogenic differentiation is critical to provoke and progress degeneration in ligaments[19,42]. Therefore, expression of SOX9 as a chondrogenic marker could be an indicator of the extent of degeneration in ligaments. Our work strongly suggests that the increased expression levels and the maintenance of Scleraxis-positive cells could be promising factors to improve the prognosis in degenerating ligaments as well as healing in injured ligaments[18]. OA is a serious clinical problem because it is a major cause of disability, particularly in older patients. It remains to be elucidated whether suppression of chondrogenic differentiation can prevent progression of the degenerative process of cruciate ligaments in patients with OA.

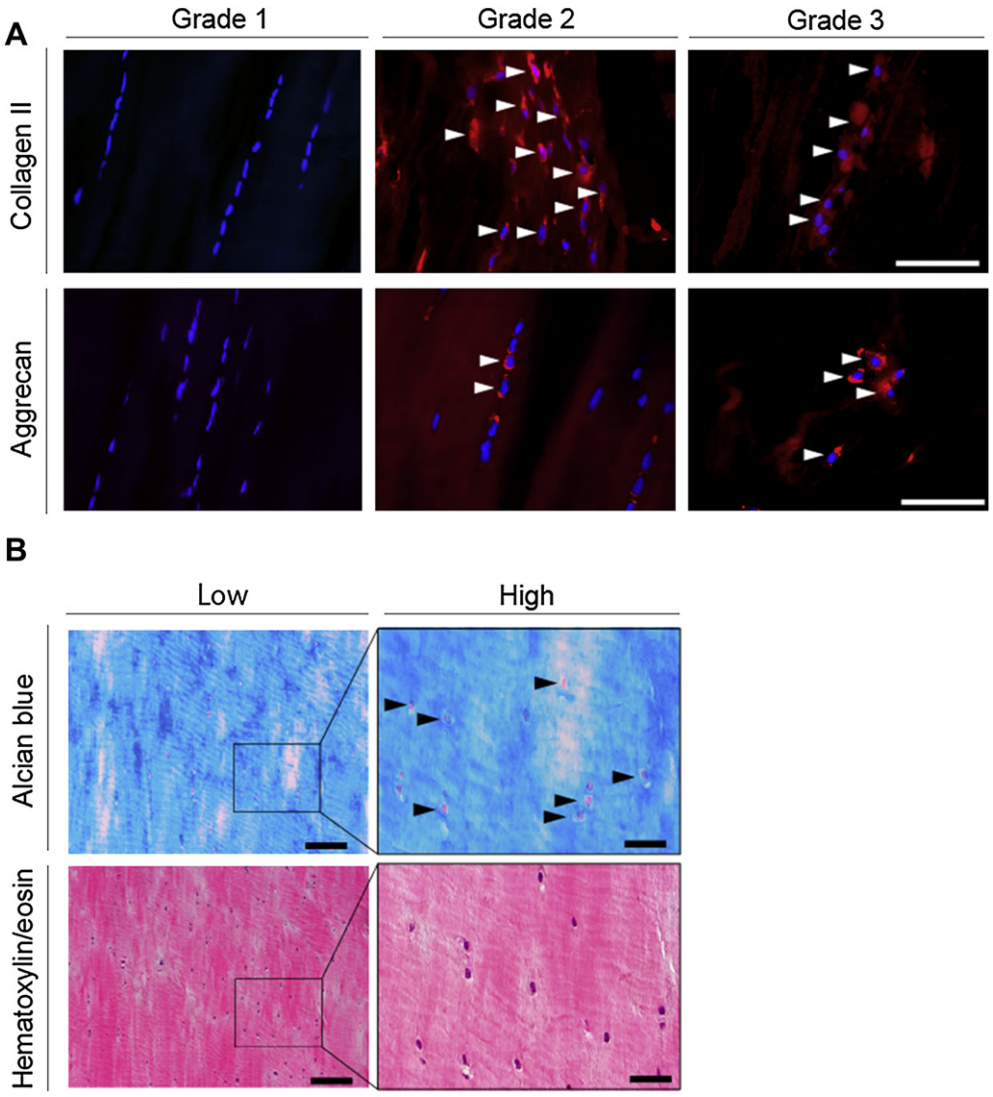

Fig. 6. Immunofluorescence staining for collagen type II and aggrecan, and Alcian blue staining in degenerating cruciate ligaments. (A) Expressions of collagen type II and aggrecan in grades 1–3. Upper panels: collagen type II (red) and nuclear staining with DAPI (blue). Lower panels: aggrecan (red) and DAPI (blue). Note that focal and scattered spot-like depositions of collagen type II and aggrecan are shown in the ECM surrounding round cells in grades 2 and 3 (arrowheads). Scale bar = 50 μm. (B) Alcian blue staining from the grade 2 sample. Upper panels: Alcian blue staining. Lower panels: hematoxylin/eosin staining. Strong reactions (blue) are evident in the ECM around round cells (arrowheads). Scale bar = 100 μm (left panels) and 25 μm (right panels).

Authors contributions

Ken Kumagai, Tomoyuki Saito, and Takao Sakai conceived ideas and designed experiments. Takao Sakai supervised the project. Ken Kumagai, Yasushi Akamatsu, and Tomoyuki Saito did provision of materials and patients. Ken Kumagai and Keiko Sakai performed experiments. Takako Sasaki generated antibodies. Ken Kumagai, Yoshihiro Kusayama, and Takao Sakai analyzed the data. Kentaro Sakamaki and Satoshi Morita performed statistical analysis. Ken Kumagai and Takao Sakai wrote and edited the manuscript.

Conflict of interest

The authors disclose no conflict of interest.

Acknowledgments

The authors thank Kimi Ishikawa for help with sample preparation. The authors also thank Dr Ronen Schweitzer (Shriners Hospital for Children, Portland, OR, USA) for Scleraxis-floxed mice, Dr Véronique Léjard (INSERM U652 and Paris-Descartes University, Paris, France) for Scleraxis cDNA, Dr Robert A. Weinberg (Whitehead Institute, Cambridge, MA, USA) for pCMV-dR8.2 dvpr and pCMV-VSV-G, and Christine Kassuba for editorial assistance. This work was supported in part by the Sumitomo Foundation, Tokyo, Japan, and Cleveland Clinic, Cleveland, OH, USA (to T. Sakai).

References

1. Nelissen RG, Hogendoorn PC. Retain or sacrifice the posterior cruciate ligament in total knee arthroplasty? A histopathological study of the cruciate ligament in osteoarthritic and rheumatoid disease. J Clin Pathol 2001; 54:381–4.
2. Allain J, Goutallier D, Voisin MC. Macroscopic and histological assessments of the cruciate ligaments in arthrosis of the knee. Acta Orthop Scand 2001;72:266–9.
3. Akisue T, Stulberg BN, Bauer TW, McMahon JT, Wilde AH, Kurosaka M. Histologic evaluation of posterior cruciate

ligaments from osteoarthritic knees. Clin Orthop Relat Res 2002;400:165–73.
4. Lee GC, Cushner FD, Vigoritta V, Scuderi GR, Insall JN, Scott WN. Evaluation of the anterior cruciate ligament integrity and degenerative arthritic patterns in patients undergoing total knee arthroplasty. J Arthroplasty 2005;20:59–65.
5. Riley G. Chronic tendon pathology: molecular basis and therapeutic implications. Expert Rev Mol Med 2005;7:1–25.
6. Loeser RF. Age-related changes in the musculoskeletal system and the development of osteoarthritis. Clin Geriatr Med 2010;26:371–86.
7. Hasegawa A, Otsuki S, Pauli C, Miyaki S, Patil S, Steklov N, *et al*. Anterior cruciate ligament changes in human joint in aging and osteoarthritis. Arthritis Rheum 2012;64:696–704.
8. Strocchi R, De Pasquale V, Facchini A, Raspanti M, Zaffagnini S, Marcacci M. Age-related changes in human anterior cruciate ligament (ACL) collagen fibrils. Ital J Anat Embryol 1996;101:213–20.
9. Wilder FV, Hall BJ, Barrett Jr JP, Lemrow NB. History of acute knee injury and osteoarthritis of the knee: a prospective epidemiological assessment. The Clearwater Osteoarthritis Study. Osteoarthritis Cartilage 2002;10:611–6.
10. Hill CL, Seo GS, Gale D, Totterman S, Gale ME, Felson DT. Cruciate ligament integrity in osteoarthritis of the knee. Arthritis Rheum 2005;52:794–9.
11. Mullaji AB, Marawar SV, Simha M, Jindal G. Cruciate ligaments in arthritic knees: a histologic study with radiologic correlation. J Arthroplasty 2008;23:567–72.
12. Tallon C, Maffulli N, Ewen SW. Ruptured Achilles tendons are significantly more degenerated than tendinopathic tendons. Med Sci Sports Exerc 2001;33:1983–90.
13. Riley GP, Harrall RL, Constant CR, Chard MD, Cawston TE, Hazleman BL. Tendon degeneration and chronic shoulder pain: changes in the collagen composition of the human rotator cuff tendons in rotator cuff tendinitis. Ann Rheum Dis 1994;53:359–66.
14. Samiric T, Parkinson J, Ilic MZ, Cook J, Feller JA, Handley CJ. Changes in the composition of the extracellular matrix in patellar tendinopathy. Matrix Biol 2009;28:230–6.
15. Cserjesi P, Brown D, Ligon KL, Lyons GE, Copeland NG, Gilbert DJ, *et al*. Scleraxis: a basic helix-loop-helix protein that prefigures skeletal formation during mouse embryogenesis. Development 1995;121:1099–110.
16. Schweitzer R, Chyung JH, Murtaugh LC, Brent AE, Rosen V, Olson EN, *et al*. Analysis of the tendon cell fate using Scleraxis, a specific marker for tendons and ligaments. Development 2001;128:3855–66.
17. Pryce BA, Brent AE, Murchison ND, Tabin CJ, Schweitzer R. Generation of transgenic tendon reporters, ScxGFP and ScxAP, using regulatory elements of the scleraxis gene. Dev Dyn 2007;236:1677–82.
18. Maeda T, Sakabe T, Sunaga A, Sakai K, Rivera AL, Keene DR, *et al*. Conversion of mechanical force into TGF-beta-mediated biochemical signals. Curr Biol 2011;21:933–41.
19. Lui PP, Fu SC, Chan LS, Hung LK, Chan KM. Chondrocyte phenotype and ectopic ossification in collagenase-induced tendon degeneration. J Histochem Cytochem 2009;57:91–100.
20. Koshino T, Machida J. Grading system of articular cartilage degeneration in osteoarthritis of the knee. Bull Hosp Jt Dis 1993;53:41–6.
21. Timpl R. Antibodies to collagens and procollagens. Methods Enzymol 1982;82(Pt A):472–98.
22. Moriya K, Bae E, Honda K, Sakai K, Sakaguchi T, Tsujimoto I, *et al*. A fibronectin-independent mechanism of collagen fibrillogenesis in adult liver remodeling. Gastroenterology 2011;140:1653–63.
23. Murchison ND, Price BA, Conner DA, Keene DR, Olson EN, Tabin CJ, *et al*. Regulation of tendon differentiation by scleraxis distinguishes force-transmitting tendons from muscle-anchoring tendons. Development 2007;134:2697–708.
24. Bolt P, Clerk AN, Luu HH, Kang Q, Kummer JL, Deng ZL, *et al*. BMP-14 gene therapy increases tendon tensile strength in a rat model of Achilles tendon injury. J Bone Joint Surg Am 2007;89:1315–20.
25. Rickert M, Wang H, Wieloch P, Lorenz H, Steck E, Sabo D, *et al*. Adenovirus-mediated gene transfer of growth and differentiation factor-5 into tenocytes and the healing rat Achilles tendon. Connect Tissue Res 2005;46:175–83.
26. Stewart SA, Dykxhoorn DM, Palliser D, Mizuno H, Yu EY, An DS, *et al*. Lentivirus-delivered stable gene silencing by RNAi in primary cells. RNA 2003;9:493–501.
27. Girgis FG, Marshall JL, Monajem A. The cruciate ligaments of the knee joint. Anatomical, functional and experimental analysis. Clin Orthop Relat Res 1975;106:216–31.
28. Amiel D, Frank C, Harwood F, Fronek J, Akeson W. Tendons and ligaments: a morphological and biochemical comparison. J Orthop Res 1984;1:257–65.
29. Rumian AP, Wallace AL, Birch HL. Tendons and ligaments are anatomically distinct but overlap in molecular and morphological features – a comparative study in an ovine model. J Orthop Res 2007;25:458–64.
30. Cheng MT, Yang HW, Chen TH, Lee OK. Isolation and characterization of multipotent stem cells from human cruciate ligaments. Cell Prolif 2009;42:448–60.
31. Wu B, Chen J, Dela Rosa T, Yu Q, Wang A, Xu J, *et al*. Cellular response and extracellular matrix breakdown in rotator cuff tendon rupture. Arch Orthop Trauma Surg 2011;131:405–11.
32. Chen J, Wang A, Xu J, Zheng M. In chronic lateral epicondylitis, apoptosis and autophagic cell death occur in the extensor carpi radialis brevis tendon. J Shoulder Elbow Surg 2010;19:355–62.
33. Cushner FD, La Rosa DF, Vigorita VJ, Scuderi GR, Scott WN, Insall JN. A quantitative histologic comparison: ACL degeneration in the osteoarthritic knee. J Arthroplasty 2003;18:687–92.
34. Woo SL, Hollis JM, Adams DJ, Lyon RM, Takai S. Tensile properties of the human femur-anterior cruciate ligament-tibia complex. The effects of specimen age and orientation. Am J Sports Med 1991;19:217–25.
35. Noyes FR, Grood ES. The strength of the anterior cruciate ligament in humans and Rhesus monkeys. J Bone Joint Surg Am 1976;58:1074–82.
36. Yuan J, Murrell GA, Wei AQ, Wang MX. Apoptosis in rotator cuff tendonopathy. J Orthop Res 2002;20:1372–9.
37. Schweitzer R, Zelzer E, Volk T. Connecting muscles to tendons: tendons and musculoskeletal development in flies and vertebrates. Development 2010;137:2807–17.
38. Tozer S, Duprez D. Tendon and ligament: development, repair and disease. Birth Defects Res C Embryo Today 2005;75:226–36.
39. Furumatsu T, Shukunami C, Amemiya-Kudo M, Shimano H, Ozaki T. Scleraxis and E47 cooperatively regulate the Sox9-dependent transcription. Int J Biochem Cell Biol 2010;42:148–56.
40. Furumatsu T, Hachioji M, Saiga K, Takata N, Yokoyama Y, Ozaki T. Anterior cruciate ligament-derived cells have high chondrogenic potential. Biochem Biophys Res Commun 2010;391:1142–7.
41. Takimoto A, Oro M, Hiraki Y, Shukunami C. Direct conversion of tenocytes into chondrocytes by Sox9. Exp Cell Res 2012;318:1492–507.
42. Clegg PD, Strassburg S, Smith RK. Cell phenotypic variation in normal and damaged tendons. Int J Exp Pathol 2007;88:227–35.